DOI: 10.1002/chem.200801922

Spectroscopy Probing of the Formation, Recognition, and Conversion of a G-Quadruplex in the Promoter Region of the *bcl-2* Oncogene

Huihui Li,[a, b] Yiquan Liu,[a] Sen Lin,[a] and Gu Yuan*[a]

Abstract: This study has demonstrated the formation of the G-quadruplex structure from the G-rich sequence in the promoter region of the *bcl-2* oncogene; the formation could be induced by addition of NH_4^+ or K^+ ions. The binding affinity and stoichiometry of seven small molecules with the G-quadruplex were examined by using ESI-MS, as well as CD and UV spectroscopy. The binding-affinity order was determined to be **P1**≈**P5**>**P2**>**P3**≈**P4**>**P7**>**P6**. In particular, the small-molecule induction of the structural transition between the G-quadruplex and duplex DNA forms in this promoter region was investigated by ESI-MS. We directly observed specific binding of dehydrocorydaline (**P7**) and cationic porphyrin (**P5**) in one system consisting of the G-quadruplex and the duplex DNA, respectively. The results indicate that **P7** selectively stabilizes the G-quadruplex and shifts the equilibrium toward G-quadruplex formation of the *bcl-2* promoter, whereas **P5** converts the G-quadruplex into the duplex DNA, which results in strong and selective binding to the duplex form. Therefore, **P5** and **P7** with their attractive binding specificities could be considered as precursors for pathway-specific drug design for regulation of *bcl-2* oncogene transcription.

Keywords: DNA structures · duplexes · G-quadruplexes · noncovalent interactions · oncogenes

Introduction

The B-cell CLL/lymphoma 2 (*bcl-2*) gene plays an essential role in cell survival. This gene has been found to be aberrantly overexpressed in some human tumors, including B-cell and T-cell lymphomas and breast, prostate, and non-small-cell lung carcinomas.[1–3] Moreover, *bcl-2* overexpression has also been found to interfere with traditional cancer therapeutics.[4] Inhibition of *bcl-2* expression by small molecules has been shown to reduce cellular proliferation and to enhance chemotherapy efficacy.[5]

The region of particular interest is the G-rich region located adjacent to the 5′-end of the *bcl-2* promoter.[6] Some transcription factors, such as Sp1, E2F, and NGF, have been found to regulate gene expression through this region.[7–9] The G-rich sequence, dGGGCGCGGGAGGAAGGGGGCGGG (S1), could form a G-quadruplex structure and act as a potential target for anticancer therapy.[10] Inside the cell, the G-rich sequence is present along with the complementary C-rich strand and, therefore, G-quadruplex structures compete with the normal Watson–Crick (WC) duplexes.[11,12] The G-quadruplex–duplex equilibrium is influenced by many factors, which involves the cellular environment, such as the pH value and available cations. This equilibrium can also be influenced by small-molecule ligands as potential anticancer agents.

Some molecules show structurally specific recognition for the G-quadruplex or duplex DNA (Scheme 1). Perylene derivatives, such as *N*,*N*-bis-(2-(dimethylamino)ethyl)-3,4,9,10-perylenetetracarboxylic acid diimide (DAPER, **P1**), favor π–π interactions with the G-tetrad surface.[13–15] The 5,10,15,20-tetrakis-(1-methyl-4-pyridyl)-21*H*,23*H*-porphine (TMPyP4, **P5**) is an effective telomerase inhibitor with an EC_{50} value of 6.5 mM in a cell-free assay; this molecule also binds to the G-quadruplex in the *c-myc* promoter.[16] Polyamides (such as ImImImβDp (**P6**)) derived from distamycin A have been extensively explored for recognition and

[a] Dr. H. H. Li, Y. Q. Liu, S. Lin, Prof. Dr. G. Yuan
Beijing National Laboratory for Molecular Sciences
Key Laboratory of Bioorganic Chemistry
and Molecular Engineering of Ministry of Education
Department of Chemical Biology, College of Chemistry and Molecular Engineering
Peking University, Beijing 100871 (China)
Fax: (+86) 10-6275-1708
E-mail: guyuan@pku.edu.cn

[b] Dr. H. H. Li
Jiangsu Key Laboratory of Biofunctional Materials
School of Chemistry and Environmental Science
Nanjing Normal University, Nanjing, 210097 (China)

Supporting information for this article is available on the WWW under http://dx.doi.org/10.1002/chem.200801922.

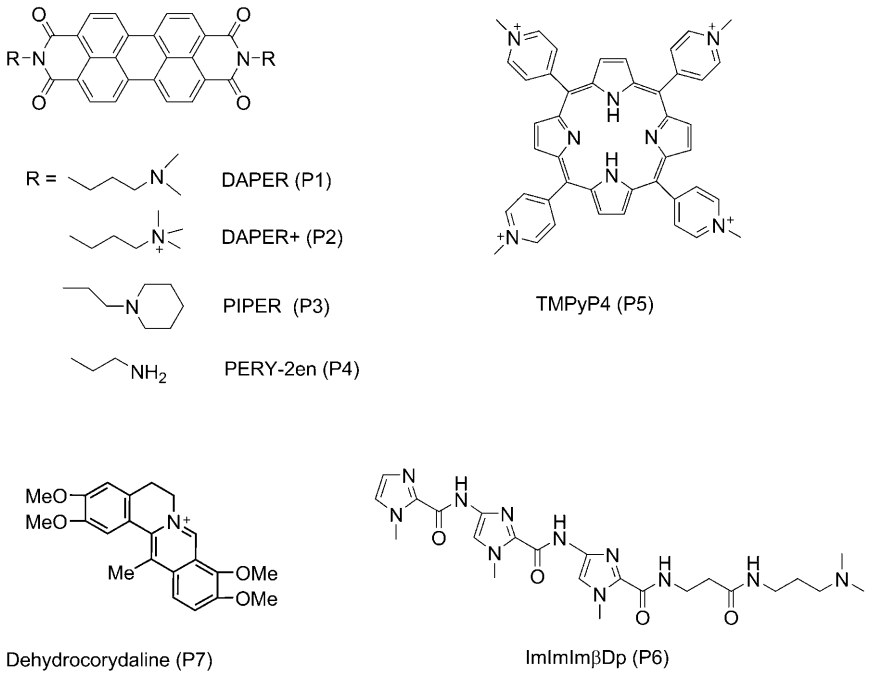

Scheme 1. Structures of the seven small molecules studied (**P1**–**P7**).

binding with high affinity in the minor groove of predetermined duplex-DNA sequences.[17,18] Recent NMR spectroscopy studies have suggested that distamycin A is also able to interact with G-quadruplex DNA.[19] With dehydrocorydaline (**P7**), a chemical constituent of Chinese traditional medicine, it is expected that π-stacking and electrostatic interactions may be present and may result in molecular-recognition properties, which would indicate good potential to bind G-quadruplexes.[20,21] To achieve therapeutic selectivity by targeting G-quadruplexes, it is necessary to understand the transition of the G-quadruplex–duplex equilibrium and to examine the effect of different environments on the G-quadruplex to the duplex transition. Therefore, seven molecules (Scheme 1) were used to explore the specific-recognition function for the G-quadruplex.

ESI-MS has been successfully applied to characterize G-quadruplex and duplex formation, as well as the interactions of these structures with ligands.[22,23] In this research, ESI-MS, as well as CD and UV spectroscopy, was used to assess the binding specificities of the small-molecule ligands toward the target G-quadruplex. In addition, the thermodynamic stability of the G-quadruplex was determined in the presence and absence of the small molecules with high binding affinity, and the induction of the equilibrium transfer between the duplex and G-quadruplex DNA by small molecules was probed.

Results and Discussion

Formation of the G-quadruplex in the *bcl-2* promoter: The ESI mass spectrum of the G-rich sequence (S1) in a 20 mM ammonium acetate solution shows a dominant peak for the G-quadruplex ion with two NH_4^+ ions, $[S1+2NH_4^+-7H^+]^{5-}$ (Figure 1). Since cations are known to sit between two G-tetrad layers and to stabilize the G-quadruplex structure, it would be reasonable to assume that there are three tetrad layers in a G-quadruplex possessing two NH_4^+ ions.[24]

The CD spectra provided additional support for the existence of the G-quadruplex structure. The CD spectrum does not give an obvious absorption at 200–350 nm for the G-rich sequence (S1) in the absence of cation (Figure 2). However, the CD spectra for S1 in ammonium acetate solution resemble most closely that

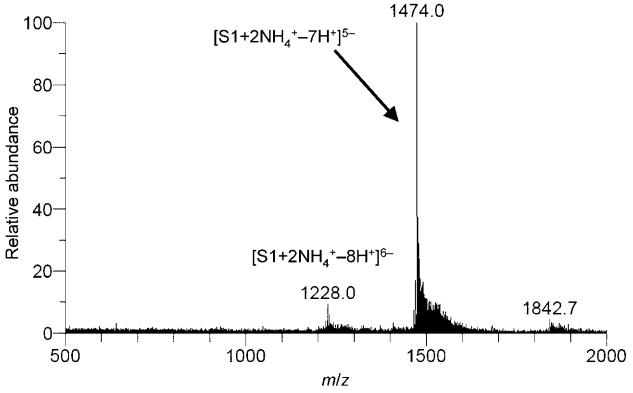

Figure 1. ESI mass spectrum of the G-rich sequence (S1) in 20 mM NH_4OAc buffer (pH 7.0).

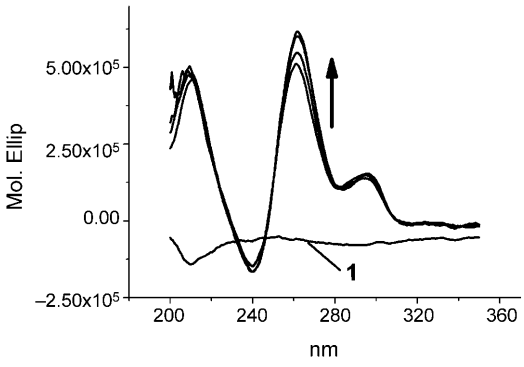

Figure 2. CD spectra of the G-rich sequence (S1) in methanol/water (25:75) (labeled 1) and NH_4OAc buffer. The arrow indicates the trend as the NH_4OAc concentration increases (5, 10, 50, and 100 mM) at pH 7.0.

in K^+ solution, in that they display an absorption maximum at 264 nm and a shoulder at 295 nm. These results confirm the formation of a mixed parallel/antiparallel G-quadruplex structure in ammonium acetate solution.[25]

To conclude, the ESI-MS and CD spectroscopy results indicated that NH_4^+ ions could induce the formation of the intramolecular G-quadruplex structure in the *bcl-2* promoter.

Complex of the G-quadruplex with small molecules: To examine the recognition specificity and stoichiometry of small molecules, such as perylene derivatives (**P*i***, $i=1$–4), the cationic porphyrin **P5**, the polyamide **P6**, and the natural product **P7**, the G-quadruplex and the corresponding small-molecule complexes were studied by mixing the target DNA with 2.5 to 40.0 μM solutions of the small molecules and measuring the ESI-MS spectra. Figure 3 shows parts of the mass spectra of the G-quadruplex DNA with two small molecules in a molar ratio of 1:4 as examples. For the cationic porphyrin **P5**, the intense signal of the 1:2 complex ion ($[G+2\,\mathbf{P5}]^{5-}$ at m/z 1737) is the base peak (Figure 3 A), and the free G-quadruplex ion is not observed in the spectrum. For **P7**, the signal of the 1:1 complex ion at m/z 1547 is the base peak, whereas the free G-quadruplex and its 1:2 complex ion have intensities of 82% and 38%, respectively (Figure 3 B). Therefore, the ESI-MS results show that **P5** has notable specificity with a 1:2 binding stoichiometry when the concentration of the small molecule reaches 40.0 μM. The ESI-MS spectra of the G-quadruplex DNA with the other small molecules at a molar ratio of 1:4 are provided in Figure S1 of the Supporting Information.

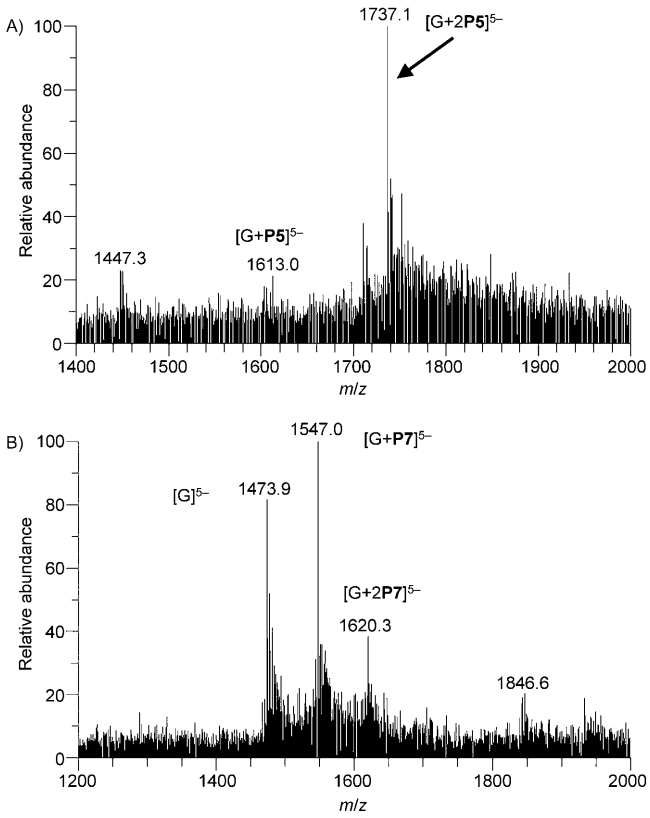

Figure 3. ESI mass spectra of 10.0 μM S1 DNA with a 40.0 μM concentration of small molecules A) **P5** and B) **P7**. [G]: G-quadruplex ion; [G+*n***P*i***]: a 1:*n* complex ion of the G-quadruplex (G) and the small molecule **P*i*** ($n=1$ or 2).

Herein, to better examine the relative binding affinities of the small molecules to the G-quadruplex ion, a parameter (IR_a) is defined as the relative intensity ratio of all complex ions to the sum of all free G-quadruplex and complex ions in the ESI spectrum [Eq. (1)]. The $\Sigma I_r(G)$, $\Sigma I_r(G+\mathbf{P}i)$, $\Sigma I_r(G+2\,\mathbf{P}i)$, and $\Sigma I_r(G+3\,\mathbf{P}i)$ values are the total intensities of the G-quadruplex (G) and the 1:1, 1:2, and 1:3 complex ions ($G+n\mathbf{P}i$), respectively. IR_a denotes the relative binding affinity for a small molecule **P*i*** with the G-quadruplex DNA.

$$IR_a = \frac{\sum I_r(G+\mathbf{P}i)+\sum I_r(G+2\,\mathbf{P}i)+\sum I_r(G+3\,\mathbf{P}i)}{\sum I_r(G)+\sum I_r(G+\mathbf{P}i)+\sum I_r(G+2\,\mathbf{P}i)+\sum I_r(G+3\,\mathbf{P}i)} \quad (1)$$

Table 1 shows the IR_a values for small molecules binding with the G-quadruplex. The results show the relative binding-affinity order of the small molecules to be **P1**≈**P5**>**P2**>**P3**≈**P4**>**P7**>**P6**. It is worth noting that the perylene derivative **P1**, with the *N*,*N*-dimethylpropyldiamine (Dp) group on the side chain, binds favorably with the target G-quadruplex structure through electrostatic interactions. However, perylene derivative **P2**, which is similar to **P1** but is further methylated at the nitrogen atom in the side chain with the consequent acquisition of a positive charge, is unfavorable for binding within the framework of DNA through electrostatic interactions.

Table 1. IR_a values for small molecules binding with G-quadruplex S1.

P*i*	Concentrationof small molecule [μM]				
	2.5	5.0	10.0	20.0	40.0
P1	0.25	0.46	0.70	0.92	0.95
P2	0.20	0.33	0.52	0.78	0.93
P3	0.26	0.30	0.38	0.64	0.86
P4	0.18	0.22	0.37	0.78	0.89
P5	0.28	0.36	0.71	0.88	0.94
P6	0.12	0.13	0.20	0.34	0.37
P7	0.16	0.25	0.37	0.58	0.74

Thermostabilization of the G-quadruplex and its complex ions: The temperature-dependent stability of the G-quadruplex and its complex ions in the gas phase was investigated with heated capillary temperatures from 60 to 400 °C.[13] The results from the G-quadruplex DNA indicated that, as the capillary temperature increased, the loss of ammonium ions from the G-quadruplex ion ($[S1+2NH_4^+-7H^+]^{5-}$ at m/z 1474) is the predominant dissociation pathway; this yields the $[S1-5H^+]^{5-}$ ion at m/z 1467. For the complex ions with small molecules, the ESI-MS spectra showed the loss of ammonium ions and small molecules and there is also a de-

crease in the intensity of the complex-ion signal as the temperature increases.

To better evaluate the different gas-phase stabilities of the G-quadruplex and its complexes with the small molecules, the novel relative intensities of the G-quadruplex ion (R_G) and the complex ion (R_C) are defined. Herein, the R_G value is the relative intensity of the sum of the G-quadruplex ion intensities ($\Sigma I_r(G)$) to the sum of the intensities of all of the G-quadruplex ions and their products with the loss of one or two ammonium ions ($\Sigma I_r(G)$, $\Sigma I_r(G-NH_3)$, $\Sigma I_r(G-2NH_3)$) in the ESI-MS spectrum [Eq. (2)]. The R_C value is the relative intensity of the sum of the intensities of the complex ions ($\Sigma I_r(G+n\mathbf{Pi})$, $n=1$–3) to the sum of the intensities of all of the complex ions and their products with the loss of one or two ammonium ions and small molecules ($\Sigma I_r(G+n\mathbf{Pi})$, $\Sigma I_r(G+n\mathbf{Pi}-NH_3)$, $\Sigma I_r(G+n\mathbf{Pi}-2NH_3)$, $\Sigma I_r(G)$) in the mass spectrum [Eq. (3)].

$$R_G(\%) = \frac{\sum I_r(G)}{\sum I_r(G)+\sum I_r(G-NH_3)+\sum I_r(G-2NH_3)} \times 100\% \quad (2)$$

$$R_C(\%) = \frac{\sum I_r(G+n\mathbf{Pi})}{\sum I_r(G+n\mathbf{Pi})+\sum I_r(G+n\mathbf{Pi}-NH_3)+\sum I_r(G+n\mathbf{Pi}-2NH_3)+\sum I_r(G)} \times 100\% \quad (3)$$

The values of R_G and R_C were calculated under the different temperature conditions by using Equations (2) and (3), respectively. The $T_{1/2}$ values are defined as the dissociation temperature at which the relative intensity of the parent ion (R_G or R_C) is reduced to the half of the initial one at 60 °C. A larger $T_{1/2}$ value implies a more stable ion, which requires a higher temperature to induce dissociation. Table 2 shows that, in the presence of **P1** and **P7**, there is a remarkable increase in the $T_{1/2}$ value of the parent ions, from 159 °C to 188 and 175 °C, respectively. By contrast, the addition of **P2** and **P5** decreases the $T_{1/2}$ value to 156 and 158 °C, respectively.

Table 2. $T_{1/2}$ and melting temperature (T_m) values for the G-quadruplex and the complexes.

	Free G	G+**P1**	G+**P2**	G+**P5**	G+**P7**
$T_{1/2}$ [°C]	159	188	156	158	175
T_m [°C]	52	60	50	54	59

A UV thermal melting study was used to obtain the T_m values for the G-quadruplex and its complexes with the small molecules. If mixed with **P1** or **P7**, the G-quadruplex complex shows a clear increase in T_m value (8 °C or 7 °C, respectively; Table 2). The thermal-stability order for binding of molecules **Pi** to the G-quadruplex is consistent with that obtained by ESI-MS. As a result, both **P1** and **P7** thermally stabilize the G-quadruplex DNA, whereas **P2** and **P5** do not contribute to the stability of the G-quadruplex DNA.

Equilibrium transfer between the G-quadruplex and the duplex DNA: Within the cell, the G-rich strands are present along with complementary C-rich strands, which generate competing duplex structures. The formation of the G-quadruplex or duplex structures relates to their relative stability. We have evaluated the stability of the G-quadruplex and its complexes with small molecules **Pi**. The equilibrium transfer between the G-quadruplex and the duplex DNA was also probed by ESI-MS and CD spectroscopy.

The ESI mass spectrum was recorded within 5 minutes after the G-rich sequence (S1) was mixed with its complementary C-rich sequence (S2: dCCCGCCCCCTTCCTCCCGCGCCC) in 50 mM NH_4OAc solution (Figure 4 A). The apparent intense peak for the G-rich sequence (S1) was that of the intramolecularly formed $[G]^{5-}$ ions at m/z 1467; this peak has around 80 % of the intensity of the base peak for the complementary C-rich sequence S2 ($[C]^{5-}$ at m/z 1350). The G-rich sequence from the *bcl-2* promoter has been confirmed to form a mix of parallel/antiparallel G-quadruplexes in ammonium acetate buffer (pH 7.0) by CD spectroscopy (Figure 2). The complementary C-rich sequence shows a positive peak at 285 nm under the same experimental conditions (Figure S2 B in the Supporting Information). The CD spectrum of an equimolar mixture of complementary sequences S1

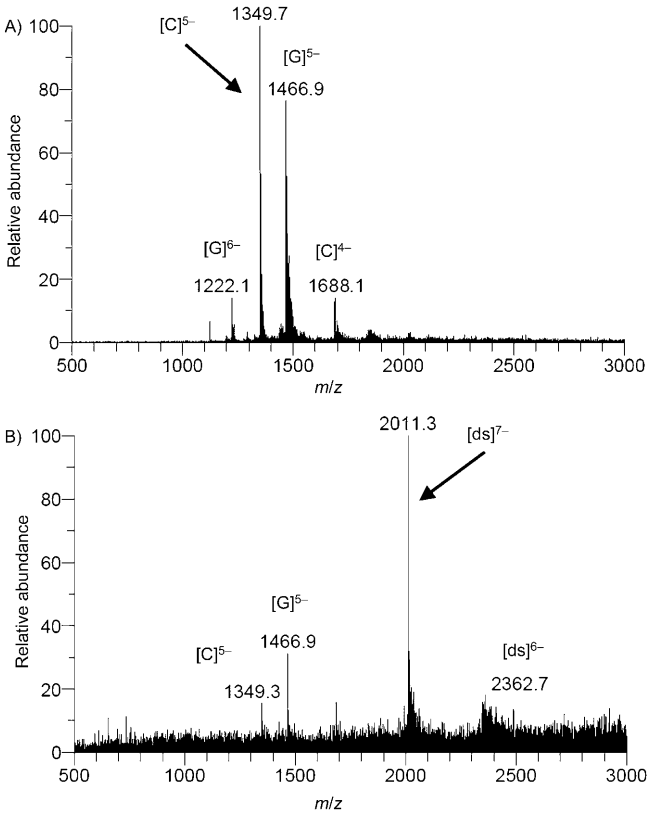

Figure 4. ESI mass spectra of the DNA solution upon mixing of the S1/S2 sequences in 50 mM ammonium acetate buffer A) for 5 min and B) for 30 min. [ds]: duplex ion.

and S2 in ammonium acetate buffer (pH 7.0) for 5 min shows a maximum at around 285 nm, with a shoulder at 264 nm and a negative peak at about 240 nm, which is the sum of the spectra for S1 and S2 DNA, as shown in Figure 5. This result implies that the 1:1 S1/S2 DNA did not

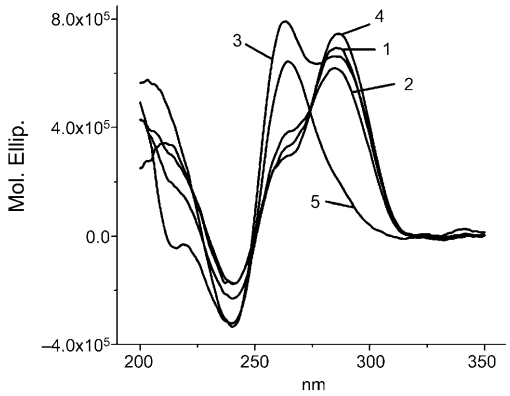

Figure 5. CD spectra in 50 mM NH_4OAc buffer at 25 °C for 1:1 mixture of the S1/S2 sequences (100 μM) left for 5 min (trace 2) or at pH 7.0, 4.0, and 10.0 for 30 min (traces 3–5), respectively; trace 1 illustrates the sum of the CD spectra of S1 and S2.

form a duplex within 5 min in ammonium acetate solution but that the G-quadruplex structure was preferentially adopted. When the DNA solution was placed for 30 min in 50 mM ammonium acetate buffer (pH 7.0), it was observed that the dominant peak changed to the duplex ion with a 7− charge ($[ds]^{7-}$ at m/z 2011), which implies that the G-rich sequence hybridizes with the complementary C-rich one, as shown in Figure 4B. Therefore, this result suggests that the *bcl-2* S1/S2 sequences undergo a structure transformation from the G-quadruplex to duplex DNA when left for 30 min.

Besides the intramolecular factors, that is, the guanine–guanine interactions, the effects of other factors, such as the pH value, DNA and NH_4OAc concentrations, the addition of organic solvents, and the interaction with the small molecules, on the interconversion between the G-quadruplex and duplex conformations were investigated.

First, the role of the pH value on the interconversion was examined between pH 4.0 and 11.0. The ESI-MS spectra show that the single-stranded ions with the 5− charge could be present as the dominant ones under acidic conditions (pH < 7.0). The CD spectrum shows a positive band at 285 nm, a shoulder peak at 264 nm, and a negative band near 240 nm at pH 4.0, which is similar to the sum of the spectra of S1 and S2 DNA, as shown in Figure 5. These results indicate that the 1:1 S1/S2 mixture at pH 4.0 did not hybridize to form the duplex but preferentially adopted the G-quadruplex structure. However, when the pH value is changed to 11.0, the equilibrium is shifted toward duplex formation. The ion corresponding to the duplex form has the base peak in the ESI mass spectrum, whereas the peak for the $[G]^{5-}$ ions decreased to less than 80% in intensity. These findings from ESI-MS and CD spectra imply that acidic conditions are favorable for duplex dissociation and the G-quadruplex formation.

Next, the influence of the DNA concentration (1–25 μM) on the interconversion of the G-quadruplex and duplex conformations was examined. The intramolecular S2 ion ($[C]^{5-}$) corresponds to the base peak (100%), and the intensity of the G-quadruplex ion ($[G]^{5-}$) is 50% in the ESI mass spectrum for 1 μM DNA. As the concentration of DNA is increased to 10 μM, the equilibrium shifts toward the duplex structure, and the base peak changed to that of the duplex ion with a 7− charge ($[ds]^{7-}$). Therefore, an increase in the concentration of DNA could induce the conformational transition from the G-quadruplex to the duplex form.

Similarly, we studied the NH_4OAc concentration dependence by considering the ESI mass spectra for the S1/S2 DNA. The results indicated that, as the NH_4OAc concentration increased from 10 mM to 200 mM, the equilibrium shifted from the G-quadruplex toward the duplex structure.

DNA is heavily packed with other molecules in the cell nuclei and this can be simulated by the presence of ethanol in solution.[26] Hence, studies performed in aqueous ethanol might provide a closer picture of the situation than those performed in water. The effect of CH_3OH, C_2H_5OH, and $(CH_3)_2CHCH_2OH$ on the DNA conformation of the S1/S2 sequences was investigated by ESI-MS. The results show that there is a notable decrease of duplex ions upon an increase of CH_3OH content from 0 to 75% in volume. The G-quadruplex ion ($[G]^{5-}$) remains nearly 60% as intense as the base peak of the single-stranded ion for the C-rich sequence ($[C]^{5-}$) in the ESI mass spectra of the DNA solution with 25–75% CH_3OH by volume. This finding implies that addition of the hydroxy compound to the DNA solution is favorable for the dissociation of the duplex structure. (The ESI mass spectra showing the effect of the three hydroxy compounds on the DNA conformation are provided in Figure S3 in the Supporting Information.)

Herein, the relative intensity ratio (R_i) of the G-quadruplex ion to the duplex ion in the ESI mass spectrum is defined as a parameter to evaluate the effects of the various factors on the interconversion of the G-quadruplex and duplex forms [Eq. (4)].

$$R_i = [G]^{5-}/[ds]^{7-} \quad (4)$$

According to Equation (4), the ratios of the relative intensities (R_i) were calculated under the different conditions. Table 3 summarizes the effects of CH_3OH, the concentration of DNA and NH_4OAc, and the pH value on the interconversion. If the value of R_i increases, this effect could be considered to induce duplex dissociation and to shift the equilibrium toward G-quadruplex formation. Acidic conditions, as well as lower concentrations of DNA and NH_4OAc, clearly lead to the stabilization of the G-quadruplex structure. The distinct behavior of CH_3OH with respect to the dissociation of the duplex DNA is remarkable.

Table 3. R_i values under different conditions.

[DNA] [μM]	R_i	CH_3OH [%]	R_i	$[NH_4^+]$ [mM]	R_i	pH	R_i
1	3.3	0	2.1	10	10.0	5	12.4
5	1.8	25	4.3	50	6.3	7	4.3
10	0.9	50	11.6	100	1.3	9	2.9
25	0.3	75	10.8	200	0.7	11	0.8

Next, we examined the role of small molecules, such as **P5** and **P7**, on the G-quadruplex to duplex transition by using ESI-MS analysis. The ESI mass spectra of mixtures of the two DNA sequences (S1/S2) with **P7** at 5 μM and 80 μM are provided in Figure S4 in the Supporting Information. The spectrum shows that the duplex ion, $[ds]^{7-}$, has the base peak in the presence of 5 μM **P7**. By contrast, addition of 80.0 μM **P7** leads to a significant change in the ESI mass spectrum, in which the base peak corresponds to the single-stranded ions of S2 ($[C]^{5-}$) and dominant peaks exist for complex ions with the G-quadruplex ($[G+\mathbf{P7}]^{5-}$ and $[G+2\mathbf{P7}]^{5-}$, respectively). It is notable that the complex ions of the G-quadruplex DNA are abundant compared with that of the duplex DNA. This indicates that **P7** preferentially binds to G-quadruplex rather than the duplex DNA and favors duplex-DNA dissociation and G-quadruplex formation.

Herein, the relative intensity ratio, IR_s, is defined as a parameter to compare the effects of the small molecules (**P*i***) on the G-quadruplex–duplex transformation. The binding selectivity of small molecules **P*i*** to the G-quadruplex and the duplex DNA could be evaluated by using the relative intensity ratio, IR_s, calculated according to Equation (5). The $\Sigma I_r(ds)$ and $\Sigma I_r(ds+n\mathbf{P}i)$ values are the total intensities of the free duplex and the duplex complexes, respectively; the $\Sigma I_r(G)$, $\Sigma I_r(G+n\mathbf{P}i)$, $\Sigma I_r(C)$, and $\Sigma I_r(C+n\mathbf{P}i)$ values are the total intensities of the free G-quadruplex, the G-quadruplex complexes, the C-rich single strand and the complexes of the C-rich single strand, respectively.

$$IR_s = \frac{\sum I_r(ds)+\sum I_r(ds+n\mathbf{P}i)}{\sum I_r(G)+\sum I_r(G+n\mathbf{P}i)+\sum I_r(C)+\sum I_r(C+n\mathbf{P}i)} \quad (5)$$

Thus, the IR_s value could be obtained for the binding selectivities of the small molecules to these different DNA forms. If the value of IR_s decreases when a small molecule is added to the equilibrium system, it implies that this small molecule could induce duplex dissociation and shift the equilibrium toward G-quadruplex formation. The IR_s values for the S1/S2 sequences binding with two small molecules (**P5** and **P7**) are summarized in Table 4 as examples. The concentrations of the small molecules were steadily increased from 5 to 80 μM, whereas the concentration of the equimolar S1/S2 sequences remained at 10 μM. As the concentration of **P7** was increased from 5 to 80 μM, the ESI-MS results showed a 23-fold decrease in the value of IR_s (from 2.3 to 0.1), which indicates a structural selectivity for G-quadruplex formation; this means that the duplex DNA was effectively converted into the G-quadruplex DNA in the presence of **P7**. By contrast, **P5** caused a steady increase in the value of IR_s from 1.5 to 13.1 as the concentration was increased from 5 to 80 μM. Therefore, **P5** converts the G-quadruplex into duplex DNA, which results in strong and selective binding to the duplex form.

Table 4. IR_s values for S1/S2 with various concentrations of **P5** and **P7**.

	Concentration [μM]					
	5	10	20	40	60	80
P5	1.5	1.9	2.6	6.4	7.4	13.1
P7	2.3	2.6	0.8	0.4	0.2	0.1

The ESI-MS profiles of the G-quadruplex and duplex forms in the absence and presence of the small molecules confirm the findings that **P7** selectively stabilizes the G-quadruplex and shifts the equilibrium toward G-quadruplex formation for the *bcl-2* promoter, whereas **P5** converts the G-quadruplex into the duplex DNA, which results in strong and selective binding to the duplex form.

To elucidate the effect of **P5** and **P7** on the equilibrium of the G-quadruplex (S1) and the duplex DNA (S1/S2) at the molecular level,[27] molecular modeling software (AutoDock3.0; see the Experimental Section) was used to calculate the lowest docked energies for the four complexes, **P7** and the G-quadruplex DNA, **P7** and the duplex DNA, **P5** and the G-quadruplex, and **P5** and the duplex DNA (Table 5); these data can be used to evaluate the different affinities.[28] The complex of **P7** and the G-quadruplex has a lower docked energy than that of the complex of **P7** and the duplex DNA. This means that **P7** has a better affinity with the quadruplex than with the duplex. However, the complex of **P5** and the G-quadruplex has a higher docked energy than that of the complex of **P5** and the duplex DNA. This means **P5** has a better affinity with the duplex DNA than with the quadruplex DNA. So if **P5** and **P7** are in system in which the G-quadruplex and duplex DNA coexist, it is most likely that **P7** pushes the equilibrium toward the G-quadruplex, whereas **P5** competes for duplex formation.

Table 5. The lowest docked energies [kcal mol^{-1}] for the complexes.

Complex	Docked energy [kcal mol^{-1}]
P7+G-quadruplex	−12.10
P7+duplex DNA	−11.35
P5+G-quadruplex	−12.79
P5+duplex DNA	−13.25

In summary, the interconversion between the G-quadruplex and duplex DNA depends on the stability of the quadruplex and its alternative duplex form, which could be influ-

enced by fluctuations in the pH value, DNA, and NH_4^+ concentrations, by addition of CH_3OH, or by the introduction of the small molecules **P5** and **P7** (Scheme 2).

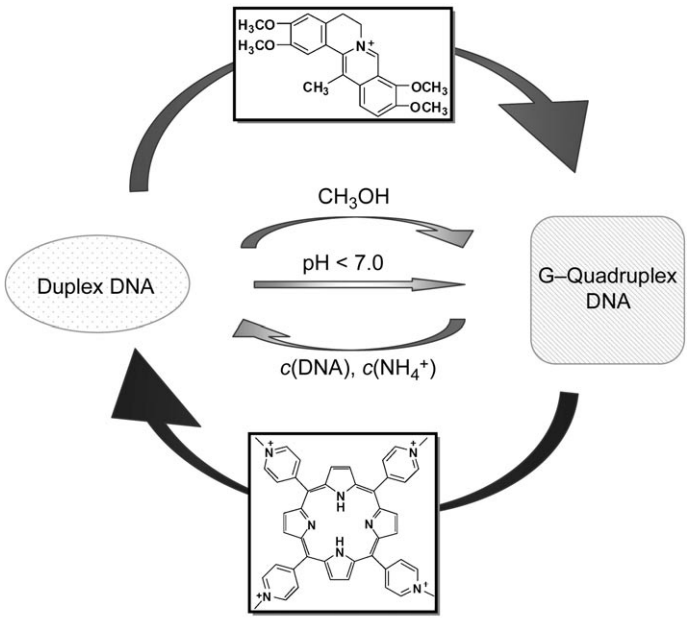

Scheme 2. Schematic map for the interconversion between the G-quadruplex and the duplex DNA in the *bcl-2* promoter.

Conclusion

This study has succeeded in probing the formation, recognition, stabilization, and conversion of the G-quadruplex in the promoter region of the *bcl-2* oncogene by ESI-MS and CD and UV spectroscopy. Both **P1** and **P7** thermally stabilize the G-quadruplex, whereas **P2** and **P5** do not contribute to the stability of the G-quadruplex DNA. The binding-affinity order of the small molecules with the G-quadruplex is **P1**≈**P5**>**P2**>**P3**≈**P4**>**P7**>**P6**. It was found that the G-quadruplex–duplex equilibrium is under the subtle influence of many factors, such as pH value and the presence of cations and small molecules. The ESI-MS and CD spectroscopy results showed that, at higher pH values or higher concentrations of DNA or cations, the *bcl-2* promoter DNA was predominantly in the duplex form. By contrast, at lower DNA or cation concentrations, under acidic conditions, and in the presence of CH_3OH, the G-quadruplex structure efficiently competes with the duplex form. In an ESI-MS study of the effects of small molecules on the G-quadruplex–duplex equilibrium, it was shown that the S1/S2 sequences related to regions of the *bcl-2* promoter preferentially adopt the G-quadruplex structure in the presence of **P7** but the duplex form predominates in the presence of **P5**.

Experimental Section

Small molecules: **P1**–**P4** and **P6** were synthesized in our laboratory.[13,14] **P5** was purchased from Sigma Chemical (St. Louis, MO). **P7** was provided by Prof. Yawei Zhou.

DNA oligonucleotides: Single-stranded oligonucleotides were purchased from Augct (Beijing, China). The abbreviation S1 was used for dGGGCGCGGGAGGAAGGGGGCGGG (M_W=7338) and S2 was used for dCCCGCCCCCTTCCTCCCGCGCCC (M_W=6751). The oligonucleotides were directly dissolved in deionized water or ammonium acetate solution; the resulting stock solution had a concentration of 400 μM DNA.

Mixing and binding assays: The small molecules were dissolved at a concentration of 100 μM in methanol/water (50:50 v/v). A 1.0 μL sample of each DNA solution was mixed with 1.0–16.0 μL of binder solution and then diluted with methanol/100 mM ammonium acetate (25:75, v/v) to a volume of 40 μL (final concentration was 10 μM for each DNA).[29,30]

Mass spectrometry: Normal ESI mass spectra were obtained in the negative-ion mode with a Finnigan LCQ Deca XP Plus ion-trap mass spectrometer (San Jose, CA). The direct-infusion flow rate was 2.0 μL min^{-1}. The electrospray-source conditions were 2.7 kV spray voltage and 120 °C capillary temperature. In all experiments, the scanned mass range was set at 500–4000 u.

Circular dichroism: The CD spectra of DNA were measured by using a J-810 spectropolarimeter (JASCO Co., Ltd., Japan) with a 0.1 cm pathlength quartz cell at 25 °C. The total concentrations of all DNA samples were 10 μM.

UV thermal melting study: UV thermal dissociation data were obtained on a Varian CARY 1 spectrophotometer equipped with a Peltier temperature controller.

Docking: **P5** and **P7** were individually docked into G-quadruplex DNA (S1) and duplex DNA (S1/S2) by using the software AutoDock3.0.[31–33] The initial G-quadruplex structure was acquired from the Protein Data Bank (PDB accession code: 2f8u). The genetic algorithm was used as the search method in docking. All of the default parameters in AutoDock3.0 were used.

Acknowledgements

This project was supported by the Research Fund for the Doctoral Program of Higher Education. We thank Mr. Jian Yuan of Dartmouth College for helpful discussions and his contribution in writing the paper. Prof. Yawei Zhou and Prof. Xinhua Wan are thanked for providing dehydrocorydaline and for performing the circular dichroism spectroscopy.

[1] J. M. Adams, S. Cory, *Science* **1998**, *281*, 1322–1326.
[2] M. L. Cleary, S. D. Smith, J. Sklar, *Cell* **1986**, *47*, 19–28.
[3] G. B. Baretton, J. Diebold, G. Christoforis, M. Vogt, C. Muller, K. Dopfer, K. Schneiderbanger, M. Schmidt, U. Lohrs, *Cancer* **1996**, *77*, 255–264.
[4] B. Desoize, *Anticancer Res.* **1994**, *14*, 2291–2294.
[5] T. Oltersdorf, S. W. Elmore, A. R. Shoemaker, R. C. Armstrong, D. J. Augeri, B. A. Belli, M. Bruncko, T. L. Deckwerth, J. Dinges, P. J. Hajduk, M. K. Joseph, S. Kitada, S. J. Korsmeyer, A. R. Kunzer, A. Letai, C. Li, M. J. Mitten, D. G. Nettesheim, S. Ng, P. M. Nimmer, J. M. O'Connor, A. Oleksijew, A. M. Petros, J. C. Reed, W. Shen, S. K. Tahir, C. B. Thompson, K. J. Tomaselli, B. L. Wang, M. D. Wendt, H. C. Zhang, S. W. Fesik, S. H. Rosenberg, *Nature* **2005**, *435*, 677–681.
[6] R. L. Young, S. J. Korsmeyer, *Mol. Cell. Biol.* **1993**, *13*, 3686–3697.
[7] C. Heckman, E. Mochon, M. Arcinas, L. M. Boxer, *J. Biol. Chem.* **1997**, *272*, 19609–19614.

[8] C. Gomez-Manzano, P. Mitlianga, J. Fueyo, H. Y. Lee, M. Hu, K. B. Spurgers, T. L. Glass, D. Koul, T. J. Liu, T. J. McDonnell, W. K. A. Yung, *Cancer Res.* **2001**, *61*, 6693–6697.
[9] Y. Z. Liu, L. M. Boxer, D. S. Latchman, *Nucleic Acids Res.* **1999**, *27*, 2086–2090.
[10] J. Dai, D. Chen, R. A. Jones, L. H. Hurley, D. Yang, *Nucleic Acids Res.* **2006**, *34*, 5133–5144.
[11] L. H. Hurley, R. T. Wheelhouse, D. Sun, S. M. Kerwin, M. Salazar, O. Y. Fedoroff, F. X. Han, H. Han, E. Izbicka, D. D. Von Hoff, *Pharmacol. Ther.* **2000**, *85*, 25 141–158.
[12] C. C. Hardin, T. Watson, M. Corregan, C. Bailey, *Biochemistry* **1992**, *31*, 833–841.
[13] H. H. Li, G. Yuan, *J. Am. Soc. Mass Spectrom.* **2008**, *19*, 550–559.
[14] J. Zhou, G. Yuan, *Chem. Eur. J.* **2007**, *13*, 5018–5023.
[15] O. Y. Fedoroff, M. Salazar, H. Han, V. V. Chemeris, S. M. Kerwin, L. H. Hurley, *Biochemistry* **1998**, *37*, 12367–12374.
[16] A. Rangan, O. Y. Fedoroff, L. H. Hurley, *J. Biol. Chem.* **2001**, *276*, 4640–4646.
[17] P. B. Dervan, R. W. Burli, *Curr. Opin. Chem. Biol.* **1999**, *3*, 688–693.
[18] M. L. Kopka, C. Yoon, D. Goodsell, P. Pjura, R. E. Dickerson, *Proc. Natl. Acad. Sci. USA* **1985**, *82*, 1376–1380.
[19] A. Randazzo, A. Galeone, V. Esposito, M. Varra, L. Mayol, *Nucl. Nucl.* **2002**, *30*, 535–545.
[20] T. S. Wu, Y. L. Leu, C. S. Kuoh, S. D. Jiang, C. F. Chen, K. H. Lee, *J. Chin. Chem. Soc.* **1997**, *44*, 357–359.
[21] C. L. Chen, H. M. Chang, E. B. Cowl, *Phytochemistry* **1976**, *15*, 547–550.
[22] C. L. Mazzitelli, J. S. Brodbelt, J. T. Kern, M. Rodriguez, S. M. Kerwin, *J. Am. Soc. Mass Spectrom.* **2006**, *17*, 593–604.
[23] N. V. Anantha, M. Azam, R. D. Sheardy, *Biochemistry* **1998**, *37*, 2709–2714.
[24] F. Rosu, V. Gabelica, C. Houssier, P. Colson, E. De Pauw, *Rapid Commun. Mass Spectrom.* **2002**, *16*, 1729–1736.
[25] T. S. Dexheimer, D. Sun, L. H. Hurley, *J. Am. Chem. Soc.* **2006**, *128*, 5404–5415.
[26] M. Vorlýckova, K. Bednarova, J. Kypr, *Biopolymers* **2006**, *82*, 253–260.
[27] N. Kumar, S. Maiti, *Nucleic Acids Res.* **2005**, *33*, 6723–6732.
[28] M. F. Sanner, *J. Mol. Graphics Modell.* **1999**, *17*, 57–61.
[29] K. X. Wan, T. Shibue, M. L. Gross, *J. Am. Chem. Soc.* **2000**, *122*, 300–307.
[30] V. Gabelica, E. De Pauw, F. Rosu, *J. Mass Spectrom.* **1999**, *34*, 1328–1337.
[31] D. S. Goodsell, A. J. Olson, *Proteins Struct. Funct. Genet.* **1990**, *8*, 195–202.
[32] G. M. Morris, D. S. Goodsell, R. Huey, A. J. Olson, *J. Computer-Aided Molecular Design* **1996**, *10*, 293–304.
[33] G. M. Morris, D. S. Goodsell, R. S. Halliday, R. Huey, W. E. Hart, R. K. Belew, A. J. Olson, *J. Comput. Chem.* **1998**, *19*, 1639–1662.

Received: September 18, 2008
Published online: January 20, 2009

